

**SIDEROPHILE ELEMENT ABUNDANCES IN Fe-S-Ni-O MELTS SEGREGATED FROM PARTIALLY MOLTEN ORDINARY CHONDRITE UNDER DYNAMIC CONDITIONS.** T. Rushmer<sup>1</sup>, M. Humayun<sup>2</sup> and A. J. Campbell<sup>2</sup> <sup>1</sup>Department of Geology, University of Vermont, Burlington, VT 05405 (tracy.rushmer@uvm.edu) <sup>2</sup>Geophysical Sciences, The University of Chicago, Chicago, IL, 60637 (hum8@midway.uchicago.edu).

**Introduction:** Early differentiation in evolving planetesimals likely involved a variety of different physical mechanisms. Fe-rich metallic liquid segregation can occur in a solid, partially molten, or purely molten silicate body, with or without the presence of deformation. Deformation may assist the segregation of low degree metallic melts. Segregation of Fe-S-Ni liquids formed by variable degrees of partial melting of chondrites imparts distinct geochemical signatures on the composition of the resulting metal. These chemical signatures vary according to initial parent body composition, segregation mechanisms and the degree to which early S-rich, and possibly O-rich, core-forming liquids were extracted. In addition, the presence of deformation may enhance both kinetics and efficiency of the physical segregation process. To explore the relationship between core formation scenarios and geochemistry, the siderophile element compositions of metals formed during deformation experiments on the Kernouvé H6 ordinary chondrite were determined by laser ablation ICP-MS [1]. We present results on siderophile concentrations in Fe-S-Ni-O quench and associated Fe-Ni metal dynamically segregated at different degrees of partial melting, and determine partition coefficients for different solid metal/liquid metal compositions as a function of temperature, strain rate and amount of silicate melt present. Further, the IIE irons are related to H chondrites by their oxygen isotope composition [2], and were argued to have formed by solidification of melts on the H chondrite parent body [3]. We apply our data to evaluate this hypothesis.

**Experimental study and Analytical approach:** Experiments were conducted on solid cores of Kernouvé H6 chondrite, 0.6" long and 0.25" in diameter, using a Griggs rock deformation apparatus. The Kernouvé cores (KM) were heated and pressurized to run conditions, then deformed while partially molten. Temperatures (T) are given for the center of the charge, but T is higher in the lower part of the charge due to a temperature gradient; details are given in [4].

Laser ablation ICP-MS analyses of individual large metal grains from Kernouvé starting mate-

rial were given in [5]. Quench Fe-S-Ni of different compositions and associated residual Fe-Ni metal from four KM experiments were analyzed using a spot size varying between 25-50  $\mu\text{m}$ . Peaks monitored included  $^{31}\text{P}$ ,  $^{33}\text{S}$ ,  $^{57}\text{Fe}$ ,  $^{59}\text{Co}$ ,  $^{60}\text{Ni}$ ,  $^{63}\text{Cu}$ ,  $^{69}\text{Ga}$ ,  $^{74}\text{Ge}$ ,  $^{75}\text{As}$ ,  $^{182}\text{W}$ ,  $^{185}\text{Re}$ ,  $^{192}\text{Os}$ ,  $^{193}\text{Ir}$ , and  $^{197}\text{Au}$ . Hoba IVB, Filomena IIA and NIST SRM1263a were used as standards [1-4].

**Results:** KM-10 (P=1.0 GPa, T=925°C, strain rate= $10^{-5}/\text{s}$ , 40% strain) contained no silicate melt, and areas of quench Fe-S-Ni-O in high stress cataclastic domains were present in the lower portion of the charge. Earlier analyses in a sheared Fe-Ni vein and from unmodified zones [3] located in the center and upper portions of the charge showed that the highly strained metal did not differ significantly from starting Kernouvé metal concentrations. New analyses in the cataclastic zone provided data on both solid metal and quench Fe-S-Ni-O compositions (23.8 wt% S, green lines in Fig 1). The data are shown in Fig. 1 ordered according to their compatibility in the solid metal-liquid metal system [6], with the most compatible (Ir) on the left.

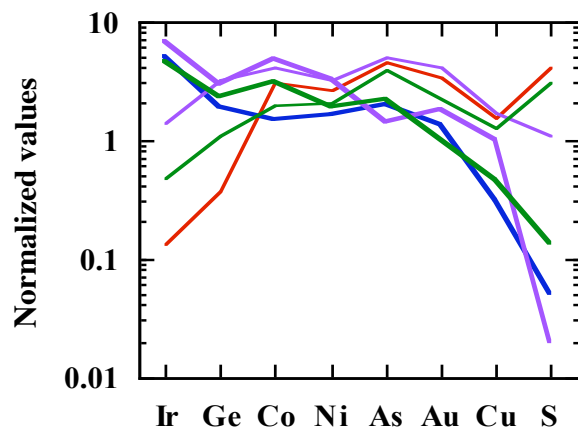


**Figure 1:** Siderophile abundances of solid metal (heavy lines) and associated quench Fe-S-Ni-O (thin lines) normalized to Fe and H chondrite compositions.

Similarly, analyses of Fe-S-Ni-O quench metal in veins and pools and associated residual metal have been collected in KM-12 (P=1.2 GPa, T=900°C, strain rate= $10^{-6}/\text{s}$ , no silicate

melt present, 10% strain, red line), in KM-11 (P=1.0 GPa, T=990°C, strain rate=10<sup>-5</sup>/s, 15-18% silicate melt present, 15% strain, purple lines) and KM-17 (P=1.2 GPa, T=940°C, strain rate=10<sup>-6</sup>/s, 12% silicate melt present, 10% strain, blue line). Previous KM-17 data were shown in [5] and show good reproducibility. Data for Fe and Ga are not shown in Fig. 1, as these are distributed between metal and silicate phases. Abundances of P, W, Re and Os were obtained in some analyses, but are not shown in Fig. 1. We note that the O content of the Fe-S-Ni liquids varies in the different experiments and the varying redox state will likewise influence e.g. S contents and Ni and Co relationships. Deformation enhances reaction kinetics in the experiments and allows us to analyze segregated liquid from residual metal in the natural samples. The results do show excellent agreement with equilibrium solid metal-liquid metal partition coefficients determined on S-bearing systems [6]. Partition coefficients have been calculated from residual metal (SM) and the associated quench (LM) compositions in the different experiments. Figure 2 gives examples of the effect of sulfur on the  $D_{SM/LM}$  values. The red diamonds in Fig. 2 are from KM-12, which contains the highest estimated sulfur quench compositions (29.6 wt% S), from the lowest degree Fe-S-Ni-O partial melt at T=900°C. The black squares in Fig. 2 are from KM-11, which shows the lowest sulfur quench composition (~6.0 wt% S) from the highest degree Fe-S-Ni-O partial melt at T=990°C.

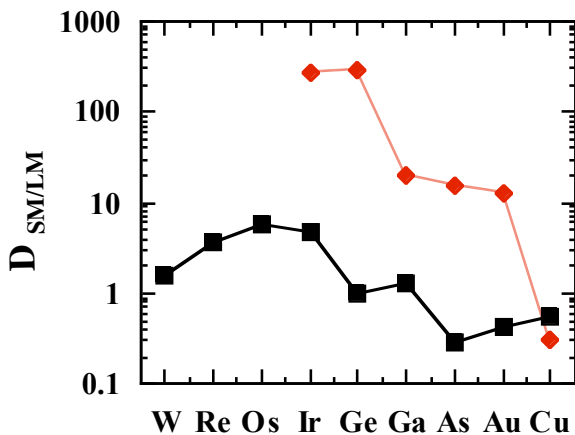


**Figure 2:**  $D_{SM/LM}$  for selected siderophile elements in two runs containing 6 wt% S (black squares) and 29.6 wt% S (red diamonds).

Clear trends exist in the data from high to low S content. Cu partitions into the S-bearing liquid under all conditions and  $D_s$  range from 0.19 at high S contents to 0.56 at low S contents. As goes from compatible to incompatible at approximately 15 wt% S in the liquid. Ir, Ge and Ga show large changes in  $D$  as a function of S, ranging from >100 to approximately 1.0 from high to low S content but remain compatible. W and Os also remain compatible (Fig. 2).

**Discussion:** Overall, the  $D$  values in the deformation experiments agree well with those in Chabot et al., 2003 [6]. Differences lie in the values for  $D$  at high S for Ir and the temperature of the experiments. We find that the lower temperatures (at 1.0-1.2 GPa) produce Fe-S-Ni liquid compositions observed at higher T in other studies [6]. Part of the difference is likely due to the temperature gradient in the charge in addition to the different redox conditions.

New analyses of partially molten Kernouvé Fe-S-Ni supports the inference from siderophile abundances and oxygen isotopes that IIE irons were derived from partial melting of H chondrites. The results also show that high sulfur, low degree partial melts have too low Ga, Ge and Ir to form IIE irons. Intermediate degrees of partial melting, represented by melt pools and veins in KM10 and KM17, are closest in composition to IIE irons. Individual solid grains in contact with these pools have Ga, Ge and Ir contents that are high for IIE irons, indicating that the IIE irons did not form as crystal cumulates from parental liquids, but represent segregated melts or mixtures of melt+crystals. The compositional range of experimental melt compositions exceeds the observed range of IIE irons. The IIE irons represent a limited portion of the experimental Ni-Co trend, implying generation from a limited range of redox conditions.

#### References:

- [1] Campbell A. J., Humayun M. and Weisberg M. K. (2002) *GCA*, **66**, 647-660. [2] Clayton R. N. and Mayeda T. K. (1996) *GCA*, **60**, 1999. [3] Wasson J. and Wang J. (1986), *GCA* **50**, 725. [4] Rushmer, T., Minarik, W.G. and Taylor, G.J. (2000) *In: Origin of the Earth and Moon* pgs. 227-249 [5] Rushmer, T., Humayun M. and Campbell A. J. (2003) *LPSC Abs* # 1174. [6] Chabot, N., Campbell, A.J., Jones, J.H., Humayun, M. and Agee, C.B. (2003) *MAPS*, **38**, 181-196.